2021 European Control Conference (ECC)
June 29 - July 2, 2021. Rotterdam, Netherlands

Experimental Study of Aerodynamic Disturbance Rejection On Multirotor Unmanned Aerial Vehicles

Jawhar Chebbi[12] and Yves Brière[2]

***Abstract*— PID (Proportional-Integral-Derivative) controllers are the most widely used control algorithms in different industrial applications. Multirotor Unmanned Aerial Vehicles (UAVs) are not an exception in this regard. This success is due to the efficiency of this type of algorithms. In fact, they are easy to understand, to tune and to implement. Added to that, PID controllers perform surprisingly well in most operational cases, even when those start to become challenging. But this effectiveness becomes questionable when the conditions are far from being nominal as we show in this study where we compare PID with adaptive and disturbance observer-based controllers for an under-actuated multirotor. We show that, when the inertial and actuation properties of the UAV are well modelled, good disturbance rejection capabilities can be achieved by simply adding a disturbance observer to a PID controller.**

I. INTRODUCTION

Multirotor UAVs have numerous industrial applications (aerial photography, mapping, inspection, etc.) that require them to be operating autonomously in an outdoor environment. These flying robots are nonetheless too sensitive to aerodynamic disturbances, especially the under-actuated ones. This is first of all due to the very nature of their actuation which is based on aerodynamic thrust and torque generated by accelerating air through rotating blades, so the surrounding wind has a significant influence on the behaviour and performance of the rotors. Secondly, wind measurement is hard to have on this kind of vehicles because it interferes with the air re-circulation induced by the rotors, added to that most wind measurement technologies are based on static calibration (of pressure with reference to the tilt angle for example) and cannot capture the transient dynamics, this becomes even harder on under-actuated UAVs that need to constantly change their attitude to move. Furthermore, the drag force caused by the interaction with wind is hard to model because it has various forms and origins (blade flapping, induced drag, transitional drag, profile drag and parasitic drag, refer to [1] and references therein for more details). Therefore, designing a controller to withstand such disturbed conditions can be challenging. In most industrial applications, PID controllers, or slightly enhanced versions of PID, are used. And when tuned properly, reasonable performances can be achieved.

In this study, we compare a PI position controller with equivalently tuned Model Reference Adaptive (MRAC) and Active Disturbance Rejection Controllers (ADRC) during a constant wind exposure scenario. We show that the resulting performances from the latter two are comparable to the augmentation of PI with a disturbance rejection term. We then extend this analysis to the attitude dynamics, and we add a torque disturbance rejection solution allowing to reach even better performances and confirming that a substantial part of the wind disturbance acts on the UAV as a torque.

The remainder of the paper is structured as follows: firstly some relevant related work on disturbance rejection is presented, then the position control design is detailed for the different methods and some guidelines to tune them are given, and lastly the experimental results are presented and discussed.

II. LITERATURE ON DISTURBANCE REJECTION FOR UAVS

Disturbance rejection for multirotor UAVs has been widely considered using various control approaches. Most of these techniques boil down to two main ideas that depend on the error to be minimised: either a reference model tracking error or an internal open-loop model one. In the first case, learning techniques are employed (like adaptive or model predictive control) and in the latter, disturbance observers or estimators are used. More or less knowledge about the controlled system is needed in both cases. But a model for the actuators is almost always required.

Adaptive control techniques have been successfully used for multirotor UAVs to resist to internal and external disturbances. These are considered as additional uncertain parameters to be estimated. For instance, an adaptive position controller is presented in [2] and a full $SE(3)$ geometric one is developed in [3] to track an available smooth position and attitude trajectory. Several other adaptive control variants were also designed for multirotor UAVs, like L_1 adaptive control that allows faster adaptation than basic adaptive schemes while ensuring better stability margins ([4] and [5]). Model Reference Adaptive Control was also employed towards the same end in [6], [7] and [8] where some robustifying modifications were introduced.

Disturbance observers have also been successfully applied for disturbance estimation and cancellation on multirotor UAVs. The observers can take several forms, and their construction follows more or less equivalent philosophies based on an internal open-loop model. Some works in this context include the use of Extended State Observers ([9] and [10]), Extended Kalman Filters [11], Sliding Mode Disturbance Observers ([12]), Disturbance Observers ([13]

[1]Jawhar Chebbi, Donecle, Labege, France jawhar.chebbi@donecle.com
[2]Jawhar Chebbi and Yves Briere, Aerospace Vehicles Design and Control Department (DCAS), ISAE-SUPAERO, Toulouse University, France (jawhar.chebbi yves.briere)@isae-supaero.fr

and [14]), Finite-Time Convergence Disturbance Observer ([15]), Reduced-Order Disturbance Observer [16].

III. Overview of Position Control Design

The position control algorithm of a multirotor UAV generates a desired 3D thrust force $\mathbf{u}_T$ in the earth fixed frame which gives the desired thrust in the UAV body frame, along with the required tilt angle. By adding a yaw angle target, one can obtain the direction cosine matrix (noted $\mathbf{R}$) that fully describes the desired orientation of the UAV. This rotation matrix is sent to the attitude controller to use it as a reference to track. So now we only focus on computing $\mathbf{u}_T$, knowing that we can translate it into the desired orientation.

a) Assumption 1: We have of a model P_V of the actuators' behaviour allowing to transform any static thrust force T to an equivalent duty cycle PWM command u, given a battery voltage V[1], and vice versa. This model is a simple quadratic equation (for a fixed voltage) in the case of a quadrotor. But it can be more complex for other configurations to account for some aerodynamic interference between rotors, see for example the coaxial case in [17].

The uncertainty on this map is modelled as a constant multiplicative gain: $T = \omega P_V(u)$ which can be transformed to an additive one $T = P_V(u) + \delta P_V(u)$ by having $\delta = \omega - 1$

b) Assumption 2: The UAV mass is precisely known. This might be a limitation for a real application where the payload changes, but this is a different problem from the one considered in this paper which is the rejection of external disturbances[2]

c) Assumption 3: The UAV has a stable and well controlled attitude.

Considering the above assumptions, the position dynamics can be described by a linear system in the following form.

$$\begin{cases} \dot{\mathbf{p}} &= \mathbf{v} \\ \dot{\mathbf{v}} &= \boldsymbol{\mathcal{G}} + \frac{1}{m}\left(\mathbf{u}_T + \mathbf{F}_d\right) \end{cases} \tag{1}$$

The integrator dynamics are also introduced (if used within the control)

$$\dot{\mathbf{s}} = \mathbf{r} - \mathbf{p} \tag{2}$$

Where $\mathbf{r}$ is the position target, $\boldsymbol{\mathcal{G}} = \begin{bmatrix} 0 & 0 & g \end{bmatrix}^\top$ and

$$\mathbf{u}_T = \mathbf{R}\begin{bmatrix} 0 & 0 & -P_V(u) \end{bmatrix}^\top \tag{3}$$

Note that $\mathbf{F}_d$ encompasses all the force-like signals that affect the UAV body dynamics and that are not coming from the known actuators' behaviour. So this term depends also on $\mathbf{v}$ and u since it contains the drag forces and the uncertainty on the rotors' thrust model.

$$\mathbf{F}_d = \mathbf{F}_{drag}(\mathbf{v}, \mathbf{v}_{wind}) + \delta \mathbf{u}_T \tag{4}$$

However, this dependency cannot be always exploited, unless accurate drag models and wind measurements are available. It can be partially exploited when adaptive control is used as will be seen in the sequel. So for now all of these nonlinear effects are kept lumped in $\mathbf{F}_d$ in order to be able to compare the various approaches mutually.

From Equation (1) and Equation (2), position dynamics can be written in the form of a linear system of the following handy state-space form

$$\dot{\mathbf{X}} = \mathbf{A}\mathbf{X} + \mathbf{B}\left(\mathbf{u}_T + m\boldsymbol{\mathcal{G}} + \mathbf{F}_d\right) + \mathbf{E}\mathbf{r} \tag{5}$$

Where $\mathbf{X} = \begin{bmatrix} \mathbf{p} & \mathbf{v} & \mathbf{s} \end{bmatrix}^\top$ $\mathbf{A} = \begin{bmatrix} \mathbf{0}_{3\times3} & \mathbb{1}_{3\times3} & \mathbf{0}_{3\times3} \\ \mathbf{0}_{3\times3} & \mathbf{0}_{3\times3} & \mathbf{0}_{3\times3} \\ -\mathbb{1}_{3\times3} & \mathbf{0}_{3\times3} & \mathbf{0}_{3\times3} \end{bmatrix}$ $\mathbf{B} = \begin{bmatrix} \mathbf{0}_{3\times3} & \frac{1}{m}\mathbb{1}_{3\times3} & \mathbf{0}_{3\times3} \end{bmatrix}^\top$ and $\mathbf{E} = \begin{bmatrix} \mathbf{0}_{3\times3} & \mathbf{0}_{3\times3} & \mathbb{1}_{3\times3} \end{bmatrix}^\top$ if the integrator is used. Otherwise, $\mathbf{X} = \begin{bmatrix} \mathbf{p} & \mathbf{v} \end{bmatrix}^\top$ $\mathbf{A} = \begin{bmatrix} \mathbf{0}_{3\times3} & \mathbb{1}_{3\times3} \\ \mathbf{0}_{3\times3} & \mathbf{0}_{3\times3} \end{bmatrix}$ $\mathbf{B} = \begin{bmatrix} \mathbf{0}_{3\times3} & \frac{1}{m}\mathbb{1}_{3\times3} \end{bmatrix}^\top$ and $\mathbf{E} = \mathbf{0}_{6\times3}$

The different controllers to be compared in this study fit into the following common form

$$\mathbf{u}_T = \mathbf{u}_t + \mathbf{u}_d \tag{6}$$

Where $\mathbf{u}_t$ is the control signal component insuring stability and trajectory following through feedback (and possibly feed-forward) action and $\mathbf{u}_d$ is the disturbance rejection part.

A. Proportional-Integral (PI) Position Control

We consider the design of a Proportional-Integral controller. The derivative term is implicit here because we dispose of the velocity measurement (it is present in the state $\mathbf{X}$).

$$\begin{cases} \mathbf{u}_t &= \boldsymbol{\lambda}\mathbf{r} - \mathbf{K}\mathbf{X} \\ \mathbf{u}_d &= \mathbf{0} \end{cases} \tag{7}$$

Where $\mathbf{K} = \begin{bmatrix} k_p^x & 0 & 0 & k_v^x & 0 & 0 & k_i^x & 0 & 0 \\ 0 & k_p^y & 0 & 0 & k_v^y & 0 & 0 & k_i^y & 0 \\ 0 & 0 & k_p^z & 0 & 0 & k_v^z & 0 & 0 & k_i^z \end{bmatrix}$. $\boldsymbol{\lambda} = \mathbf{diag}\left(\lambda^x, \lambda^y, \lambda^z\right)$ is chosen to make the low frequency (DC) gain of the system equal to 1, it only adds zeros to the system, so is important to shape the trajectory tracking response but has no effect on stability or disturbance rejection. And $\mathbf{u}_d$ is the disturbance rejection term which is equal to zero for PID controllers for which only the integrator term has a disturbance attenuation effect.

B. Active Disturbance Rejection Position Control (ADRC)

Active Disturbance Rejection Control has been considered as an alternative to PID. It is articulated around the idea of estimating and rejecting a lumped disturbance term. The theory behind is well described in [18]. The architecture of the controller consists of a feedback error, a feed-forward term and a disturbance rejection term obtained with an observer (classically ESO Section III-B.2). The feed-forward term is built using a Tracking Differentiator (TD) that transform a step command to a smooth reference used in the error term. So the first part of the control signal, in this case, is given by

$$\mathbf{u}_t = m\Big(\dot{\mathbf{v}}_{ref} - \mathbf{K}\left(\mathbf{X} - \mathbf{X}_{ref}\right) - \boldsymbol{\mathcal{G}}\Big) \tag{8}$$

[1]When closed-loop controlled ESC are available, there is no need to model the dependency on battery voltage, the actual rotors' RPM can be directly used to build the model of the thrust

[2]This internal uncertainty does affect the performances of the different controllers and the adaptive one is the most suited to deal with it.

Such that

$$\mathbf{K} = \begin{bmatrix} k_1^x k_2^x & 0 & 0 & k_2^x & 0 & 0 \\ 0 & k_1^y k_2^y & 0 & 0 & k_2^y & 0 \\ 0 & 0 & k_1^z k_2^z & 0 & 0 & k_2^z \end{bmatrix} \tag{9}$$

and $\mathbf{X}_{ref} = \begin{bmatrix} \mathbf{p}_{ref} & \mathbf{v}_{ref} \end{bmatrix}^\top$ is generated by a Tracking Differentiator (TD) using the setpoint $\mathbf{r}$.

The disturbance rejection part $\mathbf{u}_d$ is computed by an observer.

1) Disturbance Observer DO: The design of disturbance observers is thoroughly described in [19]. Its main idea is to estimate a filtered value of the actual disturbance. Starting from Equation (5), the disturbance should be equal to $\mathbf{F}_d^* = \mathbf{B}^\dagger \left(\dot{\mathbf{X}} - (\mathbf{A}\mathbf{X} + \mathbf{B}\mathbf{u}_T + \boldsymbol{\mathcal{G}}) \right)$, where $\mathbf{B}^\dagger = \begin{bmatrix} \mathbf{0}_{3\times 3} & m\mathbb{1}_{3\times 3} \end{bmatrix}$. So, assuming we can access $\dot{\mathbf{X}}$, a disturbance estimator can be simply designed as a filter on $\mathbf{F}_d^*$

$$\dot{\hat{\mathbf{F}}}_d = \mathbf{L}\mathbf{B}^\dagger \dot{\mathbf{X}} - \mathbf{L}\left(\mathbf{u}_T + m\boldsymbol{\mathcal{G}} + \hat{\mathbf{F}}_d \right) \tag{10}$$

Where $\mathbf{L}$ is the observer gain matrix (it can also be depending on the state in the nonlinear case). However $\dot{\mathbf{X}}$ (precisely $\dot{\mathbf{v}}$) is unavailable (measurements from IMU accelerometers can be used as in [20] but those are very noisy in our case), so an auxiliary variable $\boldsymbol{\eta} = \int \mathbf{L}\mathbf{B}^\dagger \dot{\mathbf{X}} dt$ is introduced and the disturbance observer is then given by

$$\begin{cases} \hat{\mathbf{F}}_d & = \mathbf{z} + \boldsymbol{\eta} \\ \dot{\mathbf{z}} & = -\mathbf{L}\mathbf{z} - \mathbf{L}\left(\mathbf{u}_T + m\boldsymbol{\mathcal{G}} + \boldsymbol{\eta} \right) \\ \boldsymbol{\eta} & = m\mathbf{L}\mathbf{v} \end{cases} \tag{11}$$

The disturbance rejection term in Equation (6) is then simply

$$\mathbf{u}_d = -\hat{\mathbf{F}}_d \tag{12}$$

Notes:

- In this linear case, $\mathbf{L}$ simply corresponds to the first order cut-off frequency (in $rad.s^{-1}$) to be applied on the actual disturbance signal.

$$\mathbf{L} = 2\pi \mathbf{diag}\left(f_x, f_y, f_z \right) \tag{13}$$

  where f_x, f_y and f_z are frequencies in Hz.
- This observer uses only velocity measurements because the force disturbance channel only affects the velocity dimension

2) Extended State Observer ESO: The key feature of ADRC is the Extended State Observer that can be seen, in its linear form, as a Luenberger observer on an integral-chain system where the disturbance is an additional state. So from Equation (1), the corresponding 3D linear ESO is formulated as follows

$$\begin{cases} \dot{\hat{\mathbf{p}}} & = \hat{\mathbf{v}} + \mathbf{L}_p \left(\mathbf{p} - \hat{\mathbf{p}} \right) \\ \dot{\hat{\mathbf{v}}} & = \frac{1}{m}\mathbf{u}_T + \hat{\boldsymbol{\Delta}}_d + \mathbf{L}_v \left(\mathbf{p} - \hat{\mathbf{p}} \right) \\ \dot{\hat{\boldsymbol{\Delta}}}_d & = m\mathbf{L}_d \left(\mathbf{p} - \hat{\mathbf{p}} \right) \end{cases} \tag{14}$$

The disturbance rejection term in Equation (6) is in this case

$$\mathbf{u}_d = -m\left(\hat{\boldsymbol{\Delta}}_d - \boldsymbol{\mathcal{G}} \right) \tag{15}$$

a) Notes:

- In this linear case, the observer gains can be directly related to a frequency as in the DO case. One solution is to compute the gains that place all the observer poles in the same location corresponding to that frequency. Which gives

$$\begin{aligned} \mathbf{L}_p &= 2\pi \mathbf{diag}\left(3f_x, 3f_y, 3f_z \right) \\ \mathbf{L}_v &= (2\pi)^2 \mathbf{diag}\left(3f_x^2, 3f_y^2, 3f_z^2 \right) \\ \mathbf{L}_d &= (2\pi)^3 \mathbf{diag}\left(f_x^3, f_y^3, f_z^3 \right) \end{aligned} \tag{16}$$

- ESO uses the position measurement, which is usually available and accurate for UAVs. Using velocity measurement and applying a MIMO Generalized ESO as in [21] makes the tuning of the observer harder and does not bring better performance.

C. Model Reference Adaptive Control (MRAC)

In the previous observer-based approaches, the disturbance is inferred from the input and output of the open-loop physical system, which makes sense because the force disturbance enters the system from the same channel as the control input (which is also a force since we dispose of a model for the rotors). The adaptive approach only focuses on the closed-loop behaviour and considers to be a disturbance everything that makes the controlled closed-loop system deviate from a predefined desired behaviour given by a reference model.

MRAC control can also be broke down to the same two parts introduced in Equation (6). The first has the same form as the PI controller Equation (7) (even if the integrator is not necessarily used, i.e. when $\mathbf{X} = \begin{bmatrix} \mathbf{p} & \mathbf{v} \end{bmatrix}^\top$).

$$\mathbf{u}_t = \hat{\boldsymbol{\lambda}}\mathbf{r} - \hat{\mathbf{K}}\mathbf{X} - m\boldsymbol{\mathcal{G}} \tag{17}$$

The parameters $\hat{\boldsymbol{\lambda}}$ and $\hat{\mathbf{K}}$ are possibly non constant, however since we are assuming that the UAV mass is known, the linear part of the position dynamics is no longer uncertain and one can use constant control parameters $\boldsymbol{\lambda}$ and $\mathbf{K}$.

Now using Equation (5), Equation (6) and Equation (17), and introducing the reference model as

$$\dot{\mathbf{X}}_m = \mathbf{A}_m \mathbf{X}_m + \mathbf{B}_m \mathbf{r} \tag{18}$$

such that $\mathbf{A}_m = \mathbf{A} - \mathbf{B}\mathbf{K} \quad \mathbf{B}_m = \boldsymbol{\lambda}\mathbf{B} + \mathbf{E}$ [3], we end up with the following error $(\mathbf{e} = \mathbf{X} - \mathbf{X}_m)$ dynamics

$$\dot{\mathbf{e}} = \mathbf{A}_m \mathbf{e} + \mathbf{B}\left(\mathbf{u}_d + \mathbf{F}_d \right)$$

And the structure of the new disturbance rejection term will depend on the way $\mathbf{F}_d$ is modelled and here any known internal structure and state dependence of the disturbance can come in handy. Let us assume that $\mathbf{F}_d$ can be written as

$$\mathbf{F}_d = \boldsymbol{\Theta}^\top \boldsymbol{\Phi}\left(\mathbf{X}, \mathbf{u}_T \right) \tag{19}$$

Such that $\boldsymbol{\Theta} \in \mathbb{R}^{3n_p \times 3}$ is an unknown bounded parameter matrix with a bounded rate of change and $\boldsymbol{\Phi} : \mathbb{R}^9 \times \mathbb{R}^3 \to \mathbb{R}^{3n_p \times 1}$ is a known regressor vector. The regressor vector

[3] These two equations allow to compute a reference model if the control gains are known and vice versa to have the ideal gains if a reference model is known, both of these approaches are used in this work

consists of basis functions that the designer expects the nonlinear terms to follow, this can be done in light of Equation (4): the drag force could be written as combination of linear and quadratic terms of the velocity. As for the unknown wind speed part in the drag force it could be treated as a constant an exogenous disturbance (since wind measurement is not available), and the uncertainty on the rotors model could also be included by adding $\mathbf{u}_T$ to the regressor. The disturbance rejection term is simply the following:

$$\mathbf{u}_d = -\hat{\mathbf{\Theta}}^\top \mathbf{\Phi}\left(\mathbf{X}, \mathbf{u}_T\right) \tag{20}$$

Leading to $\dot{\mathbf{e}} = \mathbf{A}_m\mathbf{e} + \mathbf{B}\left(\tilde{\mathbf{\Theta}}^\top \mathbf{\Phi}\right)$, where $\tilde{\mathbf{\Theta}} = \mathbf{\Theta} - \hat{\mathbf{\Theta}}$

Updating the adaptive parameters is done based on Lyapunov stability theory, it leads to the following adaptive law

$$\dot{\hat{\mathbf{\Theta}}} = \mathbf{\Gamma} \mathit{Proj}\left(\hat{\mathbf{\Theta}}, \mathbf{\Phi}\mathbf{e}^\top\mathbf{P}\mathbf{B}\right) \tag{21}$$

Where $\mathbf{\Gamma}$ is a symmetric positive-definite adaptive gain matrix (also called learning rate) that we choose diagonal and $\mathbf{P}$ is a symmetric positive-definite matrix that solves the Lyapunov equation $\mathbf{P}\mathbf{A}_m + \mathbf{A}_m^\top\mathbf{P} = -\mathbf{Q}$ where $\mathbf{Q}$ is a symmetric definite-positive design matrix. The projector operator *Proj* (defined in [22] or [23] for example) forces the estimated parameters to stay below a chosen upper limit $\hat{\theta}_{max}$. This is important to make sure the parameters stay within a known bounded domain.

One of the well-known limitations of standard MRAC is that the high gain direct adaptation laws induce oscillations when the adaptation gains $\mathbf{\Gamma}$ are increased, leading to high-frequency control inputs that can saturate actuators and excite higher-order dynamics. Several solutions exist in the literature to reduce this effect. The one we chose is the so-called optimal MRAC [24] where a damping-like term is added to the adaptation laws. This term is computed by solving an optimal control problem where the cost is the weighted long term tracking error, which results is an additive damping factor on the adaptive law defined as follows

$$\dot{\hat{\mathbf{\Theta}}} = \mathbf{\Gamma} \mathit{Proj}\left(\hat{\mathbf{\Theta}}, \mathbf{\Phi}\left(e^\top\mathbf{P} - \nu\mathbf{\Phi}^\top\mathbf{\Theta}\mathbf{B}^\top\mathbf{P}\mathbf{A}_m^{-1}\right)\mathbf{B}\right) \tag{22}$$

To our knowledge this is the first experimental validation of the optimal MRAC.

IV. Experimental Conditions

The considered system is a MK-quadrotor with the following physical characteristics.

- Mass $m = 1.5\ kg$
- Moments of Inertia $I_x = 0.015\ kgm^2$, $I_y = 0.014\ kgm^2$ and $I_z = 0.0294\ kgm^2$
- Actuators: Brushless electric motors attached to rigid fixed pitch propellers that can spin up to $5000\ rpm$ producing a maximal thrust of about $7\ N$. The Electrical Speed Controllers (ESC) operate in open loop and their dynamics can be approximated with a first-order linear model of a time constant equal to $0.1\ s$.

The position controller is implemented on a ground station computer that communicates with the UAV in offboard mode through Wi-Fi. The communication time delay is about $40\ ms$. Attitude control is embedded in a PX4 Pixhawk® Autopilot, it consists of a geometric attitude controller cascaded with a PID controller for the rates. Full pose measurements are provided by an Optitrack® motion capture system running at $50\ Hz$.

Wind disturbance is generated by 1-meter diameter fans blowing each a mean airspeed of $4\ m/s$ at a one-meter distance from the fan plane. In order to maximise the wind disturbance, three fans were placed as shown in Figure 1.

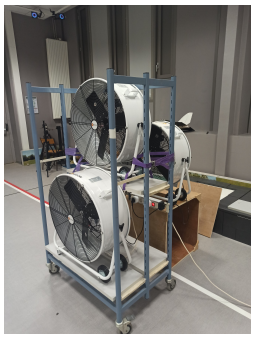

Fig. 1: Configuration of the used wind generators

In this configuration, a wind speed of about $5\ m/s$ was reached (measured using an anemometer) at a one-meter distance from the fans and a height corresponding to their centre.

V. Control Tuning

A controller's performance varies considerably with its parameters tuning. This makes comparing different controllers tricky. It is possible nonetheless to request equivalent theoretical performances from the controllers. To do so, we propose an equivalent and unified time dependent criteria on position target step response in order to allow a fair comparison between the controllers.

A. PI Controller

Let the closed-loop poles be noted for any of the three decoupled subsystems (x, y and z axes) as $-p$ and $-\omega_0\left(\xi \pm j\sqrt{1-\xi^2}\right)$. Where p, ω_0 and ξ are all positive real numbers and $\xi < 1$. We dispose then of three degrees of freedom, to make the choice easier let us set $p = \xi\omega_0$ and in this way ω_0 will determine the bandwidth of the closed-loop system. In order to set these poles, we chose $\xi = 0.9$, we are then left with one degree of liberty that we set based a time performance criterion (95% response time to a step target), we chose $tr_{95\%} = 3s$.

B. ADRC controller

The Tracking Differentiator (cf. Section III-B) allows to obtain the reference dynamics to be followed. The observer gains can be computed by choosing a cutoff frequency using Equation (16). This choice is based on a trade-off between fast estimation and measurement noise amplification. Added to noise, the time delay in the control loop leads to oscillations and adds another limit on the observer dynamics. In

our case, a good trade-off is found for a frequency equal to $1.1Hz$.

ADRC contains also feedback terms (on the tracking errors) (cf. Equation (8)). Those can also be linked to a cut-off frequency, when the structure of $\mathbf{K}$ is given by Equation (9), as $k_1^q = 4\pi\xi_t f_t$ and $k_2^q = 4\pi^2 f_t^2$, where $q \in \{x, y, z\}$, ξ_t and f_t define the damping and frequency (Hz) of the reference tracking dynamics. A good choice is to set the damping to 0.9 and the frequency to half of the one used for the observer.

C. MRAC controller

The reference model for the MRAC (and Integral MRAC) controller is chosen to achieve the same time step response given by the Tracking Differentiator (or by the PI pole placement when the integrator term is added). The choice of the adaption gain $\mathbf{\Gamma}$ is fully experimental: the value is augmented progressively until oscillations start to appear meaning that we are close to the robustness bound.

For this study, a proper adaptation behaviour value was found for $\gamma = 50$ ($\mathbf{\Gamma} = diag(\gamma)$) while introducing the optimal modification with a coefficient $\nu = 0.1$ in order to remove the oscillating behaviour and ensure robustness.

D. Conclusion

By following the tuning instructions given above, one can say that the three controllers are designed to produce equivalent performances based on time-dependent criteria. However, it is worth noticing that each algorithm has a unique characteristic: PI has the integral term, ADRC has a disturbance observer, and MRAC has nonlinear terms. So the time performance analogy made here is only approximate.

Another more adequate criteria like the norm of the applied control effort might also be considered, however the relationship with the control parameters would not be straightforward, so it cannot be used at the control design stage unless some optimisation tuning method is used. This is an interesting idea to explore in order to make the comparison fairer.

VI. Experimental Results

A simple hovering scenario is considered, the wind is blowing along the y axis, the wind fans are turned on during about 30 seconds creating a step like disturbance. The performance of the controllers is evaluated by considering the position holding capability.

A. Force Disturbance Rejection Results

The estimated force disturbance during wind application for the test scenario described above can be seen in Figure 2. Note that this estimation has a valid physical interpretation because the UAV mass and rotor's thrust are quite well known. One can also see that the drone is not perfectly centred and the force imbalance is also estimated, along with the thrust uncertainty (force on z).

Three types of criteria are used: the maximum position error MaxAE, the mean absolute position error MAE and the mean squared position error MSE.

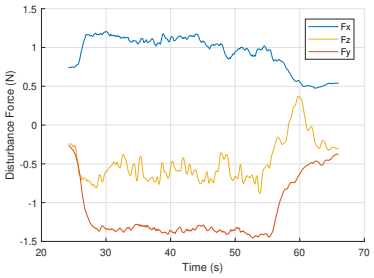

Fig. 2: Estimated force disturbance (ESO) - Fans on/off timestamps $t = 25s/55s$

The different controllers to be compared can be represented using the Venn diagram in Figure 3.

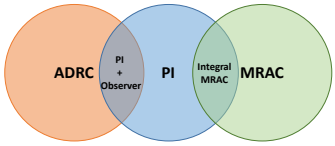

Fig. 3: Venn Diagram of the compared controllers

	PI			*ADRC*			*MRAC*		
MAE (cm)	0.94	3.58	0.53	0.88	2.16	0.85	0.45	1.72	1.02
MSE (cm)	1.13	5.25	0.72	1.13	3.68	1.23	0.55	2.69	1.29
MaxAE (cm)	2.81	15.63	2.67	3.31	16	6.38	1.86	9.50	4.01

TABLE I: Performance Comparison between PI, ADRC and MRAC ([XYZ] errors)

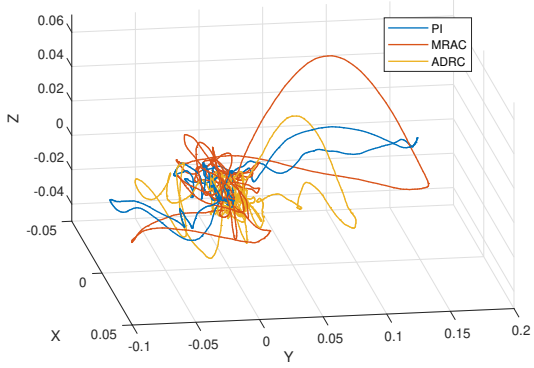

Fig. 4: Performance Comparison between PI, ADRC and MRAC - 3D Position Error

1) PI vs ADRC vs MRAC: It is interesting to see from Table I and Figure 4 that the PI controller performs better than the MRAC controller in terms of the maximum error and of the coupling induced on the disturbance-free axes (x and z).

2) Integral Term Effect: By adding an integral term to MRAC, adapting its reference model to a third-order one with the same time response, and without changing the adaptation rates, the performances are substantially improved as shows Table II. This effect of the integral term is not

surprising from a linear systems frequency analysis point of view. In fact, although the two systems have the same time response, they do not attenuate signals outside their frequency bandwidth alike. The integrator adds more attenuation at higher frequencies.

	PI			$I-MRAC$		
MAE (cm)	0.94	3.58	0.53	0.58	1.44	0.51
MSE (cm)	1.13	5.25	0.72	0.77	2.07	0.67
MaxAE (cm)	2.81	15.63	2.67	2.24	8.01	2.44

TABLE II: Performance Comparison between PI and Integral MRAC ([XYZ] errors)

3) I-MRAC vs ADRC: Both controllers lead to comparable performances as shown in Table III and Figure 5. Integral MRAC might be preferable because it leads to less coupling, although the maximum error is smaller for ADRC. It should be noted that these performances depend on the adaptation and estimation parameter values, and no clear comparison between both disturbance estimation approaches has been established in this paper.

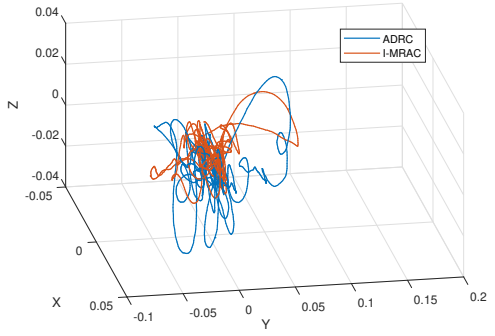

Fig. 5: Comparison between Integral MRAC and ADRC controller - 3D Position Error

	$ADRC$			$I-MRAC$		
MAE (cm)	0.50	1.518	1.01	0.58	1.44	0.51
MSE (cm)	0.65	2.23	1.27	0.77	2.07	0.67
MaxAE (cm)	2.15	7.45	3.69	2.24	8.01	2.44

TABLE III: Comparison between Integral MRAC and ADRC ([XYZ] errors)

4) Augmentation of PI: If the state-dependent terms of I-MRAC are removed, this controller can be seen as a mere augmentation of PI. So an easy alternative to MRAC or ADRC is to add a disturbance estimation term to PI. And as show Figure 6 and Table IV, it is difficult to choose the best alternative. Note that adaptive control here is not used to its full potential, namely estimating internal uncertainties. Since the system is quite well known, designing observers (based on open-loop errors) is relevant and with no surprise leads to almost the same performance as an estimator based on optimising a closed-loop error. Additionally, we notice that no obvious performance difference between using DO and ESO is seen (both are linear). ESO is preferred though because it uses position measurements that are less noisy and more accurate than velocity.

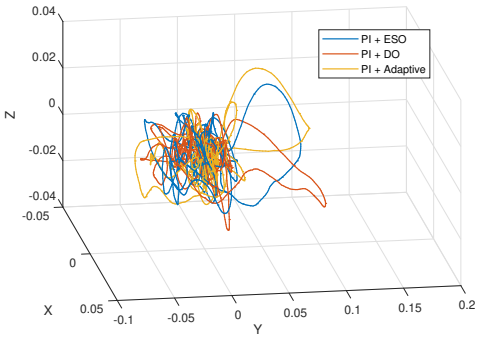

Fig. 6: Performance Comparison between Different PI Disturbance Augmentations - 3D Position Error

	$PI+ESO$			$PI+DO$			$PI+Adaptive$		
MAE (cm)	0.78	1.65	0.68	0.67	1.53	0.53	0.62	1.14	0.59
MSE (cm)	0.97	2.23	0.90	0.89	2.24	0.68	0.79	2.21	0.80
MaxAE (cm)	3.07	8.66	3.13	2.39	9.85	2.55	2.12	9.57	3.67

TABLE IV: Performance Comparison between Different Disturbance Augmentation ([XYZ] errors)

B. Torque Disturbance Rejection Results

The used wind fans do not generate a laminar aerodynamic flow, and because of the interaction with the rotors' airflow, it turns out that, in addition to forces, the multirotor is subject to torque disturbances that cannot be neglected. In light of the position control analysis, an easy and efficient torque disturbance rejection solution is to augment the used PID attitude controller with an extended state observer (assuming the inertia of the UAV is known), the results of this modification are shown here. For this comparison the PI gains were computed using $tr_{95\%} = 2s$, faster than the one used for the previous comparisons.

	PI_{pos}			$PI_{pos}+ESO_{att}$		
MAE (cm)	0.56	2.31	0.53	0.71	1.95	0.52
MSE (cm)	0.75	3.94	0.74	0.94	2.99	0.69
MaxAE (cm)	2.72	14.05	3.52	3.50	7.78	2.49

TABLE V: Comparison between PI and Integral MRAC ([XYZ] errors)

From Table V and Figure 7, it is clear that adding torque rejection to the attitude controller makes a big difference, mostly on the maximum error where about 50% improvement can be noticed. This confirms that the wind disturbance seen by the UAV consists of both force and torque components. The estimated torque disturbance during wind application is shown below Figure 8.

VII. Conclusion

A comparative experimental study between various UAV multirotor control algorithms was presented. We focused

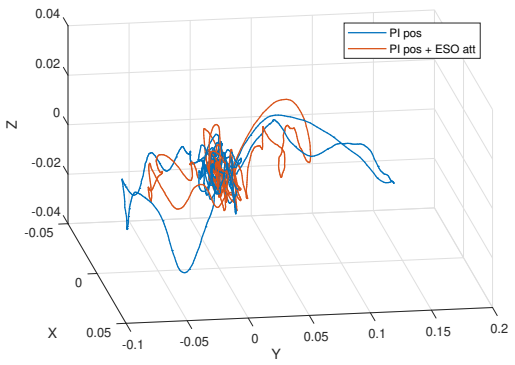

Fig. 7: Effect of Torque Disturbance Rejection - 3D View

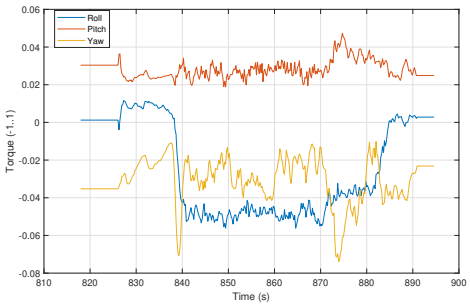

Fig. 8: Estimated torque disturbance (ESO)

on observer-based control and adaptive control, and we compared them to a baseline PI controller. The different controllers were tuned equivalently based on the same step time response criterion. The experimental results showed that adding integral action to the adaptive controller significantly improved the disturbance rejection performance. Added to that, disturbance observers appeared to bring effective disturbance rejection capabilities, mostly because the UAV system is well known, they also can be used in combination with a PID controller which brings equivalent performances to integral adaptive control. Finally, adding a disturbance observer to the attitude controller led to a significant performance improvement.

References

[1] M. Bangura, "Aerodynamics and Control of Quadrotors," PhD, The Australian National University, 2017.

[2] G. Antonelli, E. Cataldi, F. Arrichiello, P. R. Giordano, S. Chiaverini, and A. Franchi, "Adaptive Trajectory Tracking for Quadrotor MAVs in Presence of Parameter Uncertainties and External Disturbances," *IEEE Transactions on Control Systems Technology*, vol. 26, no. 1, pp. 248–254, 2018.

[3] F. A. Goodarzi, D. Lee, and T. Lee, "Geometric Adaptive Tracking Control of a Quadrotor UAV on SE(3) for Agile Maneuvers," 2014. [Online]. Available: https://arxiv.org/abs/1411.2986

[4] A. Russo, D. Invernizzi, M. Giurato, and M. LOVERA, "Adaptive Augmentation of the Attitude Control System for a Multirotor UAV," in *European Conference for Aerospace Science*, Milano, Italy, 2017. [Online]. Available: https://re.public.polimi.it/handle/11311/1045901

[5] R. A. Fernández, S. Dominguez, and P. Campoy, "L1adaptive control for Wind gust rejection in quad-rotor UAV wind turbine inspection," *2017 International Conference on Unmanned Aircraft Systems, ICUAS 2017*, pp. 1840–1849, 2017.

[6] B. Whitehead and S. Bieniawski, "Model Reference Adaptive Control of a Quadrotor UAV," in *AIAA Guidance, Navigation, and Control Conference*, no. August, Toronto, Canada, 2010. [Online]. Available: http://arc.aiaa.org/doi/10.2514/6.2010-8148

[7] M. Achtelik, T. Bierling, J. Wang, and F. Holzapfel, "Adaptive Control of a Quadcopter in the Presence of large/complete Parameter Uncertainties," in *Infotech@Aerospace*, no. March, St. Louis, Missouri, 2011.

[8] E. A. Niit and W. J. Smit, "Integration of model reference adaptive control (MRAC) with PX4 firmware for quadcopters," *2017 24th International Conference on Mechatronics and Machine Vision in Practice, M2VIP 2017*, vol. 2017-Decem, pp. 1–6, 2017.

[9] F. Yacef, N. Rizoug, L. Degaa, O. Bouhali, and M. Hamerlain, "Extended State Observer-Based Adaptive Fuzzy Tracking Control for a Quadrotor UAV," *2018 5th International Conference on Control, Decision and Information Technologies, CoDIT 2018*, pp. 1023–1028, 2018.

[10] Y. Yuan, L. Cheng, Z. Wang, and C. Sun, "Position tracking and attitude control for quadrotors via active disturbance rejection control method," *Science China Information Sciences*, vol. 62, no. 1, pp. 1–10, 2019.

[11] M. Brunner, K. Bodie, M. Kamel, M. Pantic, W. Zhang, J. Nieto, and R. Siegwart, "Trajectory Tracking Nonlinear Model Predictive Control for an Overactuated MAV," in *International Conference on Robotics and Automation ICRA 2020*, Paris, France, 2020, pp. 5342–5348.

[12] W. Cai, J. She, M. Wu, and Y. Ohyama, "Disturbance suppression for quadrotor UAV using sliding-mode-observer-based equivalent-input-disturbance approach," *ISA Transactions*, no. xxxx, 2019. [Online]. Available: https://doi.org/10.1016/j.isatra.2019.02.028

[13] K. Guo, J. Jia, X. Yu, L. Guo, and L. Xie, "Multiple observers based anti-disturbance control for a quadrotor UAV against payload and wind disturbances," *Control Engineering Practice*, vol. 102, no. July, p. 104560, 2020. [Online]. Available: https://doi.org/10.1016/j.conengprac.2020.104560

[14] J. Chen, R. Sun, and B. Zhu, "Disturbance observer-based control for small nonlinear UAV systems with transient performance constraint," *Aerospace Science and Technology*, vol. 105, p. 106028, 2020. [Online]. Available: https://doi.org/10.1016/j.ast.2020.106028

[15] M. R. Mokhtari, B. Cherki, and A. C. Braham, "Disturbance observer based hierarchical control of coaxial-rotor UAV," *ISA Transactions*, vol. 67, pp. 466–475, 2017.

[16] A. Castillo, R. Sanz, P. Garcia, W. Qiu, H. Wang, and C. Xu, "Disturbance observer-based quadrotor attitude tracking control for aggressive maneuvers," *Control Engineering Practice*, vol. 82, no. September 2017, pp. 14–23, 2019. [Online]. Available: https://doi.org/10.1016/j.conengprac.2018.09.016

[17] J. Chebbi, F. Defay, Y. Briere, and A. Deruaz-Pepin, "Novel Model-Based Control Mixing Strategy for a Coaxial Push-Pull Multirotor," *IEEE Robotics and Automation Letters*, vol. PP, no. c, p. 1, 2020.

[18] B.-Z. Guo and Z.-L. Zhao, *Active Disturbance Rejection Control for Nonlinear Systems - An Introduction*. WILEY, 2016.

[19] S. Li, J. Yang, W.-H. Chen, and X. Chen, *Disturbance Observer-Based Control: Methods and Applications*. Boca Raton: CRC Press, 2014.

[20] M. Ryll, G. Muscio, F. Pierri, E. Cataldi, G. Antonelli, F. Caccavale, D. Bicego, and A. Franchi, "6D interaction control with aerial robots: The flying end-effector paradigm," *International Journal of Robotics Research*, vol. 38, no. 9, pp. 1045–1062, 2019.

[21] S. Li, J. Yang, W. H. Chen, and X. Chen, "Generalized extended state observer based control for systems with mismatched uncertainties," *IEEE Transactions on Industrial Electronics*, vol. 59, no. 12, pp. 4792–4802, 2012.

[22] N. Hovakimyan and C. Cao, *L1 Adaptive Control Theory: Guaranteed Robustness with Fast Adaptation*. Society for Industrial and Applied Mathematics (SIAM), 2010.

[23] E. Arabi, B. C. Gruenwald, T. Yucelen, and N. T. Nguyen, "A set-theoretic model reference adaptive control architecture for disturbance rejection and uncertainty suppression with strict performance guarantees," *International Journal of Control*, vol. 91, no. 5, pp. 1195–1208, 2018.

[24] N. T. Nguyen, K. Krishnakumar, and J. Boskovic, "An optimal control modification to model-reference adaptive control for fast adaptation," *AIAA Guidance, Navigation and Control Conference and Exhibit*, pp. 1–18, 2008.